

# Non-Linear Finite Element Analysis of Flexural Reinforced Concrete Beam using Embedded Reinforcement Modeling

**Mahmud Kori Effendi**

Department of Civil Engineering, Universitas Islam Indonesia, INDONESIA

Jalan Kaliurang Km. 14,5 Yogyakarta

Corresponding author: [kori.effendi@uii.ac.id](mailto:kori.effendi@uii.ac.id)

**SUBMITTED** 09 May 2020 **REVISED** 12 June 2020 **ACCEPTED** 07 July 2020

**ABSTRACT.** Reinforced concrete is one of the most widely used building materials in Indonesia due to its workability, easiness, and reasonable price. Meanwhile, it is very important to understand the response of these elements during the loading process to ensure the development of an effective structure and one of the most effective numerical methods for reinforced concrete elements is the Finite Element Analysis (FEA). This study was, therefore, conducted to investigate the flexural behavior of reinforced concrete beam using a nonlinear finite element analysis through the application of the MSC MARC/MENTAT software program. This involved the use of a solid element to represent concrete while the truss bar was applied for reinforcing steel after which multi-linear and bilinear models were considered for the two elements respectively while embedded reinforcement model was applied to model the rebar. Moreover, the beam model was also studied and compared with experimental data from previous literature. The result showed the load-deflection to have significantly increased due to an increment in the steel reinforcement yield strength. The same was also observed for the concrete compressive strength while a decrease was recorded in deflection due to the reduction in the compressive strength because the strain was reaching the crushing value. Furthermore, the concrete tension model was found to be the same with the experimental results with the tensile strength observed to have lost its strength after reaching the tensile stress while the contact behavior of the modeled reinforced concrete beam showed the existence of a slip at the support and loading points.

**KEYWORDS** Embedded Reinforcement, Load Deflection, Non-linear, Finite Element Analysis, MSC MARC/MENTAT.

© The Author(s) 2020 This article is distributed under a Creative Commons Attribution-ShareAlike 4.0 International license.

## 1 INTRODUCTION

### 1.1 Background

The concrete reinforced (RC) with steel is extensively used in Indonesia due to its numerous advantages such as affordability, workability, and easiness and this further makes it an important material to be applied as structural elements for several constructions (Dawari and Vesmawala, 2014). It is, however, necessary to understand the response of the structural elements during loading in order to ensure the development of an effective structure. This led to the acceptance of experimental work by several researchers to investigate RC elements behavior under various loads but, despite its efficiency, it is limited by high consumption of time and funds. Therefore,

Finite Element Analysis (FEA) was introduced as one of the most effective methods to mitigate these problems in analyzing RC structural elements. It was explained to be a numerical analysis divided into smaller parts to simulate boundary conditions and static or dynamic loads in order to evaluate elements' response to these conditions (Logan, 2000).

The RC element behavior has been investigated by several researchers using finite element analysis (FEA) method. For example, Wolanski (2004) used ANSYS software to investigate the reinforced and prestressed concrete beams under

the bending load after which the experiment by Buckhouse (1997) was utilized to validate the FEA results. Moreover, the reinforcing steel inside concrete is a discrete model and has been applied in studying RC beams under two-point loading conditions (Vasudevan, Kothandaraman and Azhagarsamy, 2013) and in steel reinforcement in non-linear finite element analysis. ANSYS software was used to analyze and plot load vs deflection curves as well as crack propagation and steel yielding based on the material properties and the FEA results obtained were observed to be very close to the experimental findings. In another study, Saifullah, Nasir, and Udin (2011) investigated the nonlinear analysis of different shear reinforcements of RC beam using ANSYS for simulations and the comparison between its FEA results and a study by Wolanski (2004) showed good agreement.

Smarzewski (2016) and Dahmani, Khennane and Kaci (2010) also studied the flexural failure of reinforced concrete beams using ANSYS while Özcan et al., (2009) used the same software to investigate the nonlinear behavior of steel fiber reinforced concrete beam until the ultimate failure cracks. Furthermore, Tjitradi, Eliatun, and Taufik (2017) analyzed the bending moment capacity, deformation, stress, strain, and fracture patterns of RC beams with different types of collapsed mechanisms using 3D ANSYS model and the software was also applied by Ling *et al.* (2020) to study the effect of a hole in RC beam. Korol and Tejchman (2011) used ABAQUS to study the RC beam using an elastoplastic model with non-local softening for the concrete model while Słowik and Smarzewski (2012) applied non-linear finite element analysis using ABAQUS to determine the shear failure of reinforced concrete beams without stirrups. Moreover, Suku and Je (2020) also made use of ABAQUS in investigating the nonlinear response of the RC column with holes and the result showed the ability of a finite element to simulate experimental work with good results. The same software was also used by Suku

and Je (2020) to analyze the structural behavior of the RC frame.

This study, therefore, used nonlinear finite element analysis to investigate the flexural behavior of the RC beam under transverse loading to determine load-deflection and load-equivalent of total strain responses. The FEA model was used to analyze up to failure after which the results were compared with the experimental findings of Buckhouse (1997) which were calibrated using MSC MARC/MENTAT 2012 analysis (Öchsner and Öchsner, 2016). Moreover, Markou and Papadrakakis (2012) studied the finite element analysis of embedded steel reinforcement inside hexahedral concrete elements and the same parameters were utilized in this study to model the RC beam reinforcement using displacement control loading as the applied load. Meanwhile, contact analysis was used between concrete and steel reinforcement deformable elements as well as between concrete and surface loading plate elements.

## 2 CONSTITUTIVE MODEL FOR CONCRETE MATERIAL

### 2.1 Concrete in Compression

Element type 7 (Marc, 2012) which is an isoparametric element with eight-node and arbitrary hexahedral shape was used for concrete and, in compression, the stress was linear up to  $0,3 f_c$  and multi-linear  $f_c$  as shown in Fig. 1. The data were obtained from a concrete compressive test with a value of  $f_c=33,1$  MPa, crushing strain at 0.003, and the Poisson's ratio was 0.3. Moreover, the yield used the Linear Mohr-Coulomb failure criterion with the kinematic hardening rule while the shear retention factor applied to the isotropic concrete material was 0,5.

### 2.2 Tensile Behavior of Concrete

The concrete cracking stress in tension affected the nonlinear behavior of the reinforced concrete beam with the elastic-brittle material model assumed to be in tension. In this model, the

concrete strength reduces to zero after such cracking stress has been reached. The dashed line in Fig. 2 indicates the loss of strength by concrete after reaching tensile stress which is achieved by making  $E$  value equal to zero.

### 3 CONSTITUTIVE MODEL OF STEEL

#### 3.1 Flexural and Stirrup Steel Reinforcement

The steel material was made with reference to the element type 9 (Marc, 2012) to be a two-node and straight truss element which is used independently or in conjunction with any 3-D element. The isotropic material was also observed to be linear up to yield stress ( $f_y$ ) and bilinear up to ultimate stress ( $f_u$ ) as shown in Figure 3 while the yield criterion is Linear Mohr-Columb with isotropic hardening rule. The yield stress was defined as 413 MPa and the hardening modulus was 1000 MPa.

#### 3.2 Steel Plate at Support

The steel plate material was made with reference to the type 7 element (Marc, 2012) which is only applied at the support. This involved the use of elastic elements with a modulus of elasticity for the steel ( $E_s$ ), and the Poisson's ratio (0.3) while surface elements were used for steel plate at the loading.

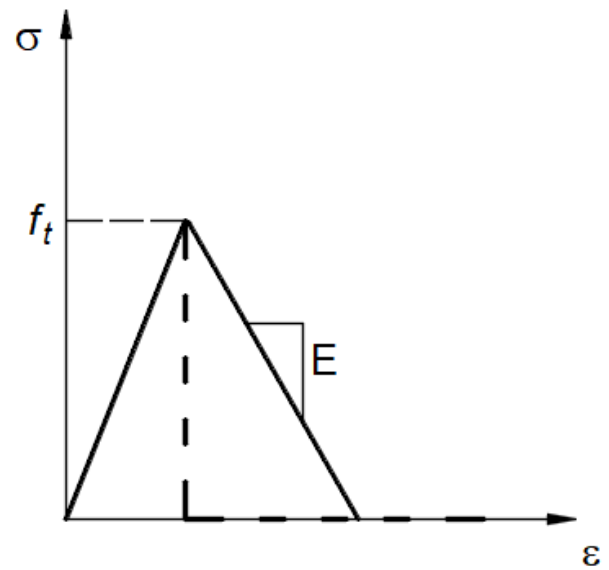


Figure 2. Brittle tension stiffening model.

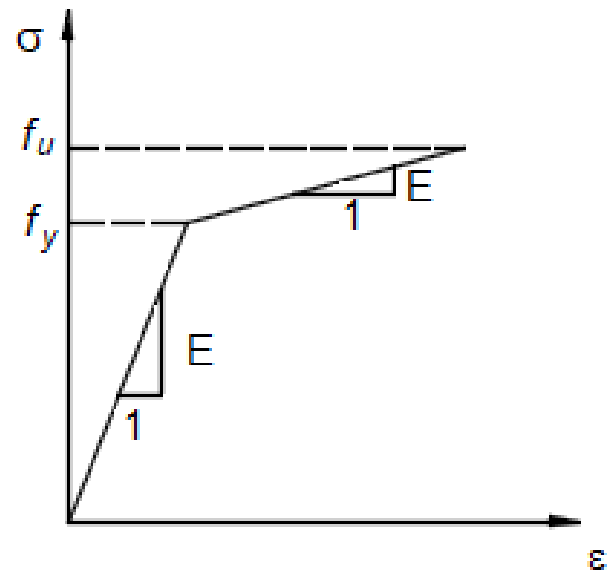


Figure 3. Uniaxial stress-strain relation for steel.

#### 3.3 FE Modeling of Steel Reinforcement

There are three techniques in modeling steel reinforcement for reinforced concrete in finite element and these include discrete, embedded, and smeared models as indicated in Figure 4 (Tavárez, 2001). The discrete model presented in Figure 4a uses sharing nodes between concrete and reinforcement elements which occupied the same region. The weakness of this model is the limitation of the concrete mesh by the reinforcement.

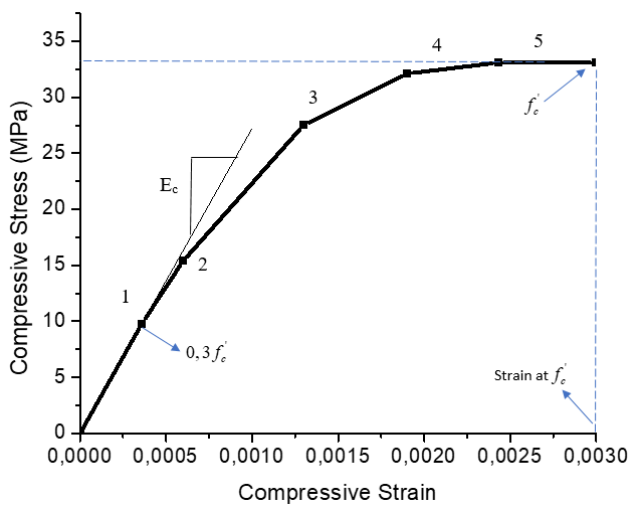


Figure 1. Stress-strain curve for concrete in compression (Kachlakev et al., 2001).

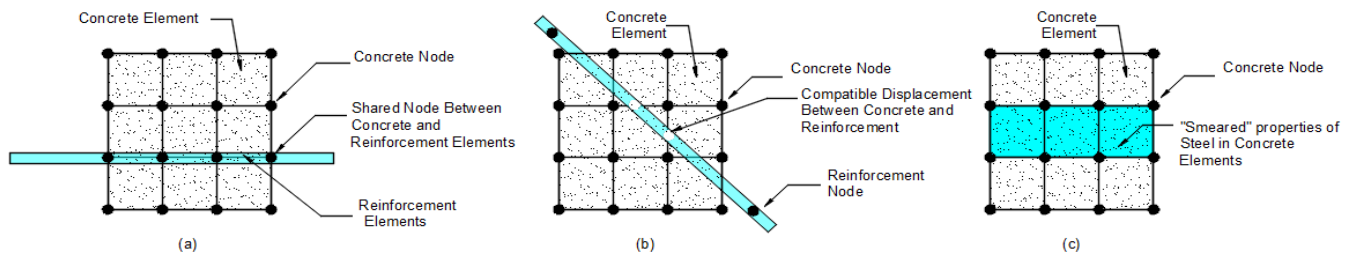


Figure 4. (a) discrete (b) embedded and (c) smeared models.

The embedded model shown in Figure 4b does not use sharing nodes between concrete and steel reinforcement and the stiffness of each material is evaluated separately due to the displacement compatibility of concrete and steel at different nodes. The model is considered effective for complex steel reinforcement but consumes time due to the presence of several nodes and degrees of freedom.

The smeared model indicated in Figure 4c is a simple assumption in the reinforcement model which spreads uniformly across all concrete elements in the area determined from the FE mesh. It is most effective in a case where the reinforcement does not contribute significantly to the overall response of the structure.

## 4 FINITE ELEMENT ANALYSIS

### 4.1 Geometry of the Beam

The experimental reinforced concrete beam was retrieved from Buckhouse (1997) in Wolanski (2004) while the FEA results in the study were also used to verify the present research. The properties of concrete and steel are the same as in Wolanski (2004) with the unit converted to the SI unit. The section of the beam was 254 mm wide and 457 mm high with a total length of the span being 4572 mm as shown in Figure 5. The beam

was simply supported with two-point loading and the reinforcement details are shown in Figure 6.

### 4.2 Material Property

The MSC MARC/MENTAT (Marc, 2010a) requires the stress-strain relationship of material to be inputted in the FEA model and the concrete material in compression was multi-linear isotropic while those in tensile regions were linear isotropic with the strength lost after the tensile stress has been attained. Meanwhile, the steel reinforcement material was bilinear isotropic while the steel plate was linear isotropic. Moreover, the failure for concrete material made use of linear Mohr-Coulomb with kinematic hardening rules while steel reinforcement materials used Von Mises criteria with isotropic hardening rules. The stress-strain relationship for concrete in compression is shown in Figure 1 while the parameters of the steel and concrete material models are highlighted in Table 1. Furthermore, solid element type 7 (Marc, 2010b) used for the proper modeling of the concrete and steel plates has eight nodes with three degrees of freedom in each which was translated in the nodal direction  $x$ ,  $y$ , and  $z$  while the truss element type 9 (Marc, 2010b) assigned to steel reinforcement is a 2D/ 3D truss element with two nodes and three degrees of freedom also translated in  $x$ ,  $y$ , and  $z$ . This element is also capable of undergoing plastic deformation.

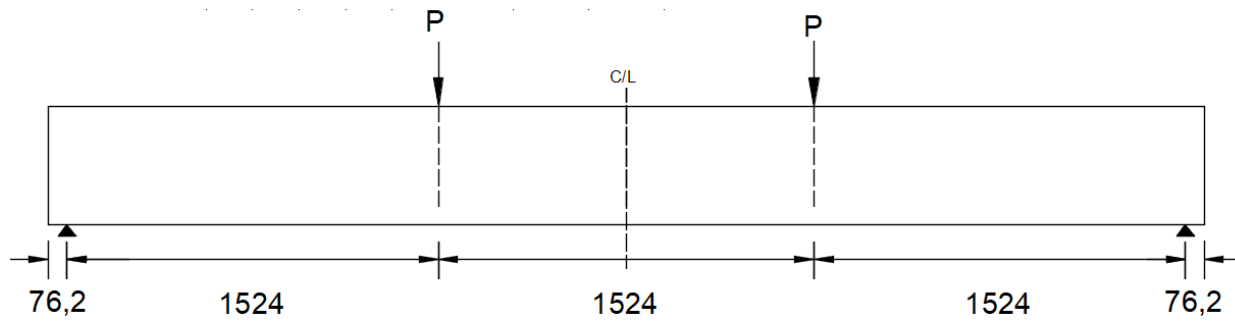


Figure 5. Geometry of the beam for FEA study.

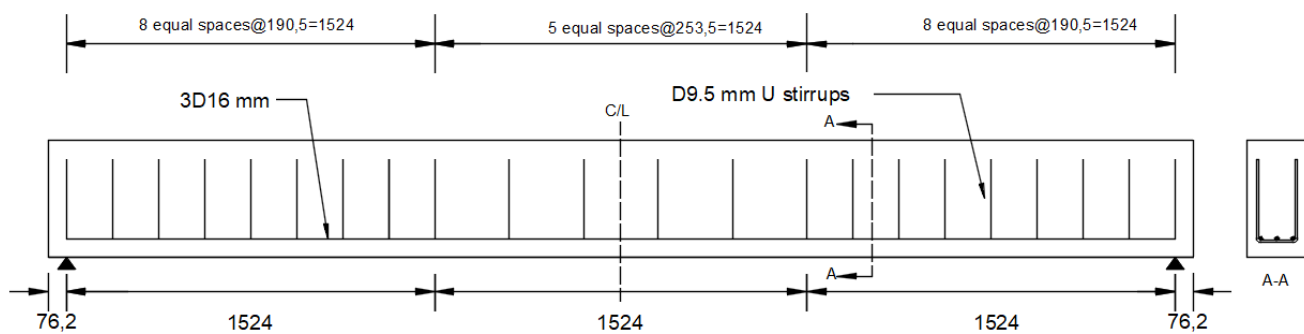


Figure 6. Typical details for RC beam reinforcement.

Table 1. Material Properties of FEA Model

Material	Element Type	Material Properties	
Concrete	Type 7	Linear Isotropic	
		$E$	27227 MPa
		$\nu$	0.3
		Multi-linear Isotropic	
		Strain	Stress MPa
		0.00036	9.8
		0.0006	15.4
		0.0013	27.5
Steel Reinforcement	Type 9	Linear Isotropic	
		$E_s$	199948 MPa
		$\nu$	0.3
		Bilinear Isotropic	
		Yield stress	413 MPa
		Ultimate Stress	620 MPa
Steel Plate	Type 7	Linear Isotropic	
		$E_s$	199948 MPa
		$\nu$	0.3

### 4.3 Finite Element Modeling

Only a quarter of the beam was modeled due to symmetry in order to save computation time and the support made use of a  $76.2 \times 127 \times 25.4$  mm steel plate while the plate at the load point was  $152.4 \times 127 \times 25.4$  mm. The combined volumes of the plate, support, and beam are shown in Figure 7. Moreover, as previously stated, solid type 7 element of MSC Marc/Mentat was used for both concrete and steel plate with the meshing set up to be rectangular and a very small gap created between the elements to ensure they do not share nodes as shown in the overall mesh of the concrete and support volumes in Figure 8. A truss element type 9 was used to create flexural and shear reinforcement and a plane of symmetry were observed to be existing for reinforcement and concrete, therefore, one half of the normal area for D15.875 mm rebar was used because one half has been cut off and the beam half of the stirrup was modeled throughout for shear reinforcement. Furthermore, the rebar was discovered to be sharing the same nodes at the points of intersection with the shear stirrups as illustrated in Figure 9(a) while the embedded reinforcement elements were allocated inside the hexahedral concrete elements as shown in (b).

Meanwhile, the steel reinforcements were modeled as a discrete model (Wolanski, 2004).

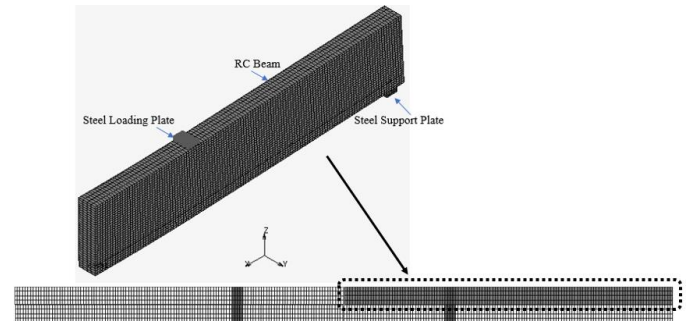


Figure 7. Volumes created in MSC MARC/MENTAT.

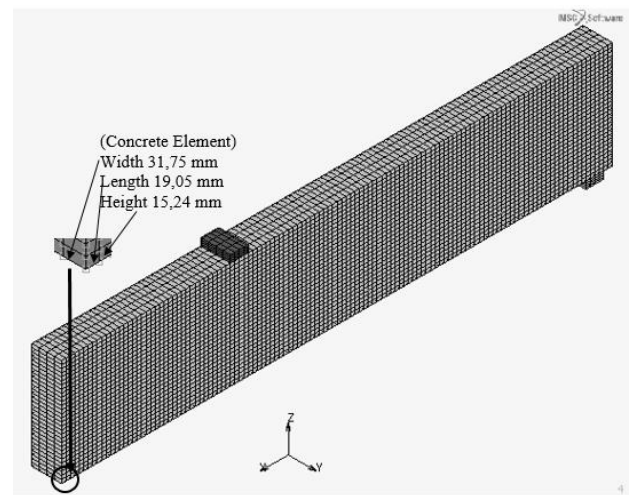


Figure 8. Concrete and steel support meshes.

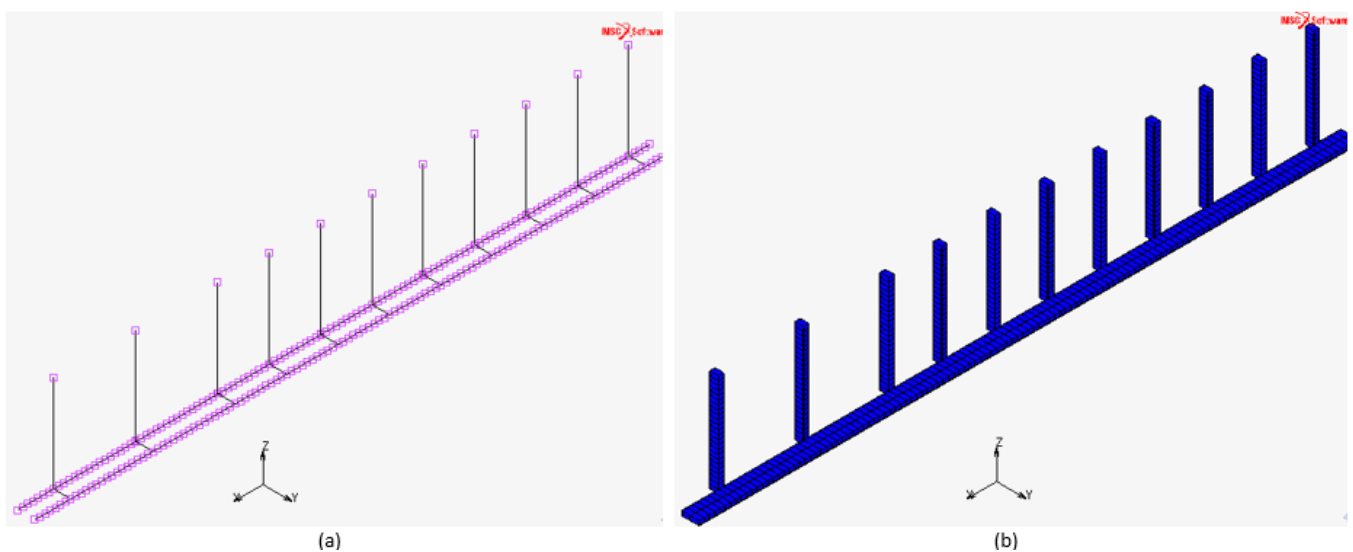


Figure 9. Reinforcement configuration. (a) Detailed (b) Embedded model

#### 4.4 Contact Conditions

The experimental work showed the existence of contact phenomena between the concrete and loading plate as well as with the steel support plate. This was observed with the deformable bodies of concrete touching the deformable steel support while the rigid bodies of the loading plate touched the deformable bodies of concrete as shown in Figure 10. In line with the contact table in MSC MARC MENTAT, the contact pairs were set and default parameters used in the table were applied in the present study. Meanwhile, this analysis was not conducted in Wolanski (2004) due to the node shared by the concrete and steel plates.

#### 4.5 Loads and Boundary Conditions

The load and boundary conditions of the FEA model were set to be the same with the experimental beam and this involved having a double symmetry plane. Only a quarter of the beam was, however, modeled in the analysis to save computation time. All the nodal translation degrees of freedom on  $X$  direction were restrained,  $u = 0$ , to model the  $Y$ - $Z$  plane symmetry while those on  $Y$  direction were also restrained,  $v = 0$ , for  $X$ - $Z$  plane. Moreover, the support was observed to be modeled basically as a pin-roller with all degrees of freedom constrained in the line of nodes for the support except at  $Y$ -direction where it was allowed to rotate. The applied load,  $P$ , was controlled by increasing the downward vertical displacement of the steel plate's surface elements. The load and boundary conditions are, however, shown in Figure 10.

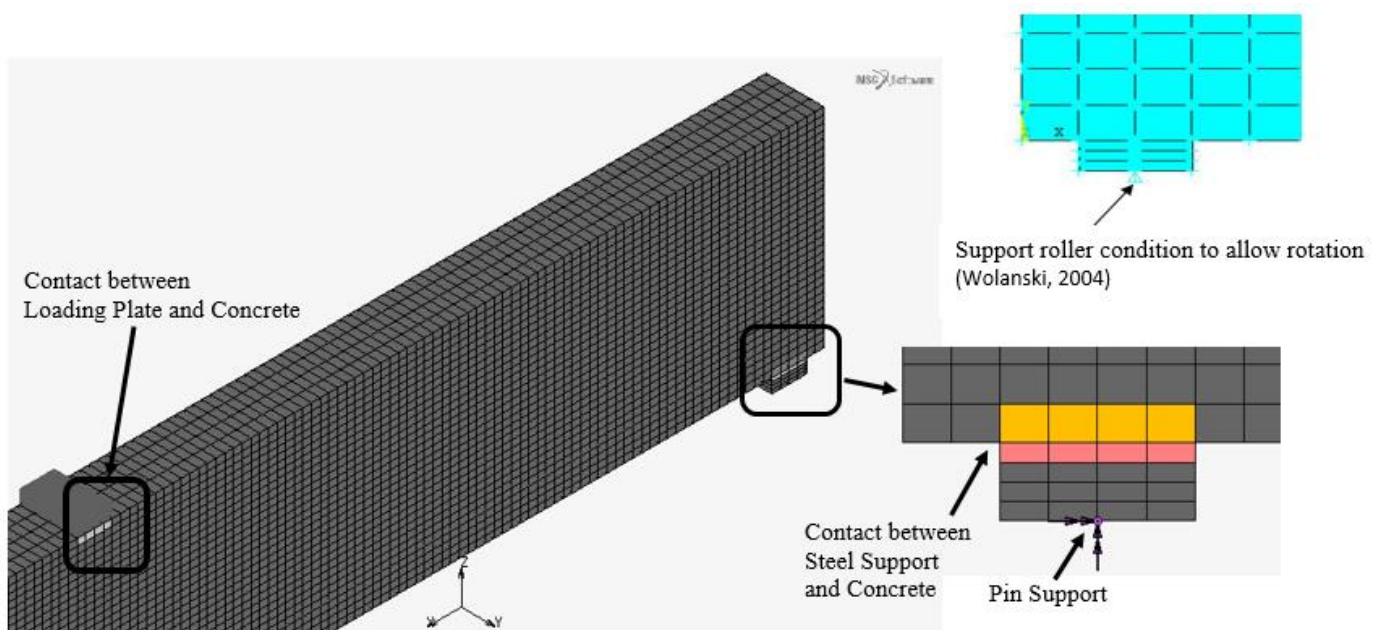


Figure 10. Contact analysis

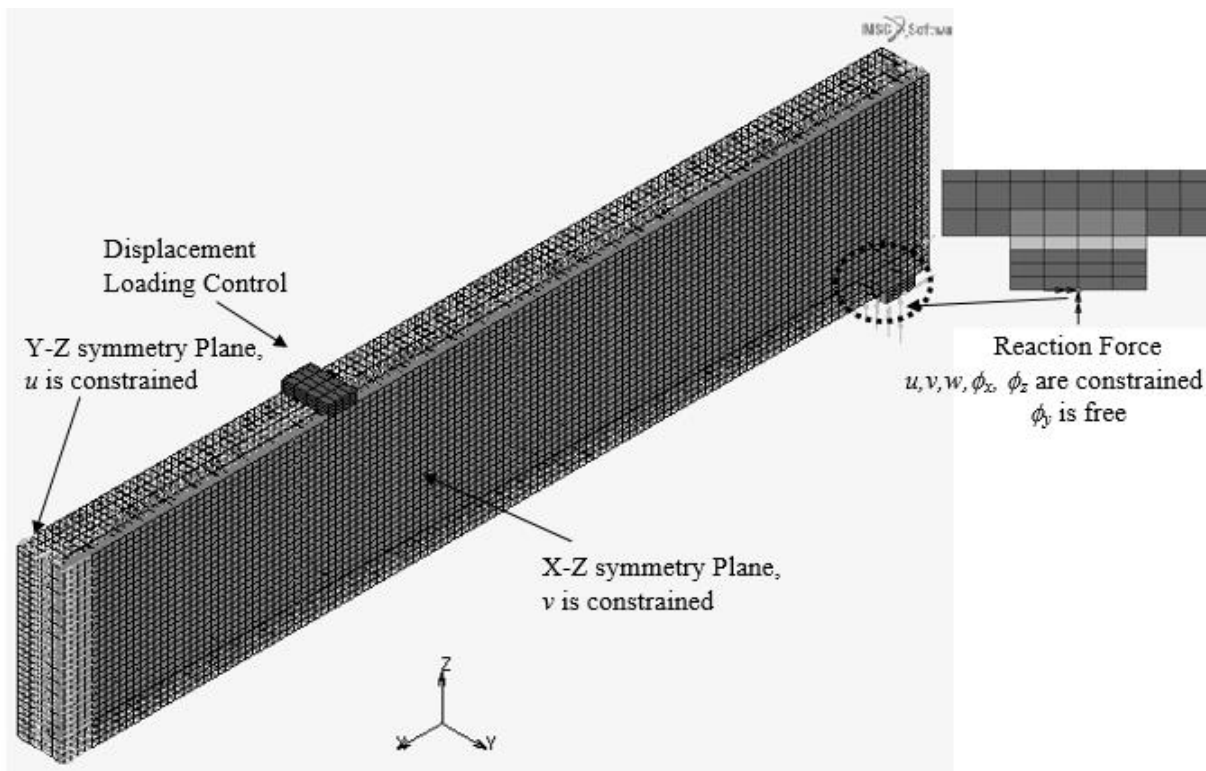


Figure 11. Load and boundary conditions

## 5 RESULTS AND DISCUSSIONS

### 5.1 Load-Deflection Response

A quarter of the RC beam with the load versus mid-span deflection curve from the experiment and FEA presented in Figure 12. The load was obtained by summing the reaction force in the line nodes of the support elements after which it was multiplied by 2 due to symmetry and applied to incrementally displace the surface elements downward. The mid-span deflection was measured from the bottom center of the beam with both force and displacement convergence set to 0.1 to solve the nonlinear equation. The load-deflection curve was observed to be trilinear including before the beam cracked, before the steel reinforcement yielded, and at the ultimate state of the beam. The first crack load was estimated at 15 kN which is smaller than the theoretical value of 23.3 kN as shown in the Appendix and this small value is probably due to the convergence criteria which were set at the default value up to the first crack load (Halahla, 2019). A small kink was also recorded in the FEA

at load 15 kN while the maximum load and maximum deflection at mid-span were 74 kN and 93.4 mm, respectively which are observed to be very close to the 72 kN and 92.7 mm recorded in the experiment. Meanwhile, the values for the maximum loads are both higher than the theoretical ultimate load which was found to be 61.5 kN as shown in the Appendix. The load-deflection response of the model is shown in Figure 12 to be similar to the response in Buckhouse (1997) and this means the FEA is reliable enough to be used in modeling the RC beam.

### 5.2 Tensile Strain-Displacement Response

Figure 13 shows the equivalent total strains for both flexural rebar and concrete against the displacement at the bottom mid-span of the RC beam model and the constant strain in the concrete was found to have occurred up to 15 mm deflection after which it started to increase.

Meanwhile, the maximum equivalent total strain for the concrete was recorded to be lower than the strain in steel reinforcement which linearly increased up to 15 mm deflection. At this point, the steel reinforcement started strain hardening and was constant up to 32 mm deflection and this was observed to be due to the yielding process of the reinforcement. Moreover, this yielding strain value was found to be smaller than the theoretical value ( $\epsilon_y = f_c/E_s = 0,002$ ) and, after hardening, the strain started to increase again.

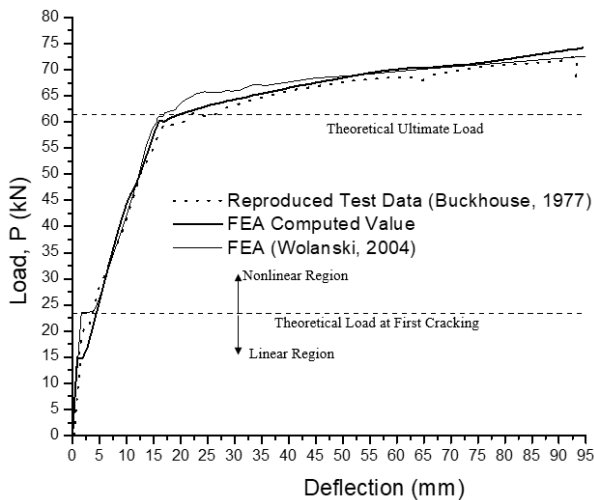


Figure 12. Load-deflection response.

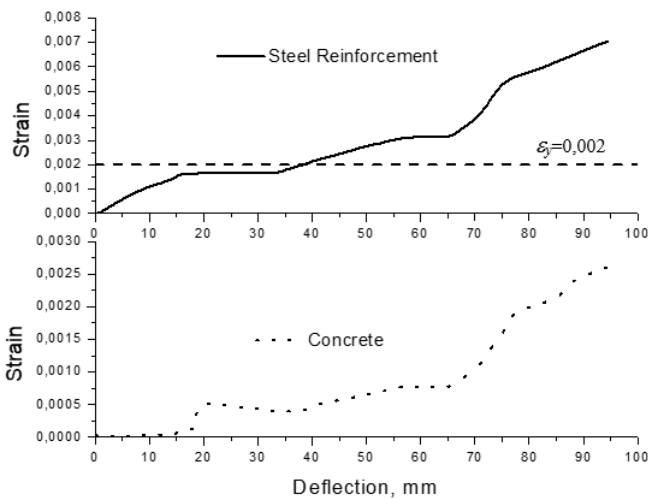


Figure 13. Equivalent total strain.

### 5.3 Contact Behavior

The slip behavior of the model is presented in Figure 14 based on the contact analysis between concrete and support as well as the loading plate. Figure 14 (a) shows the surface elements of the

loading plate were pushed down the RC beam with the loading moving vertically to ensure the plate only touches the corner of the deformed concrete and this indicates the occurrence of contact at this location. Moreover, a slip was observed between the support plate and the concrete as presented in Figure 14 (b) with the nodes of the two elements found to have displaced each other to show they are not shared and this further indicates the RC beam was placed on the plate support in the experiment.

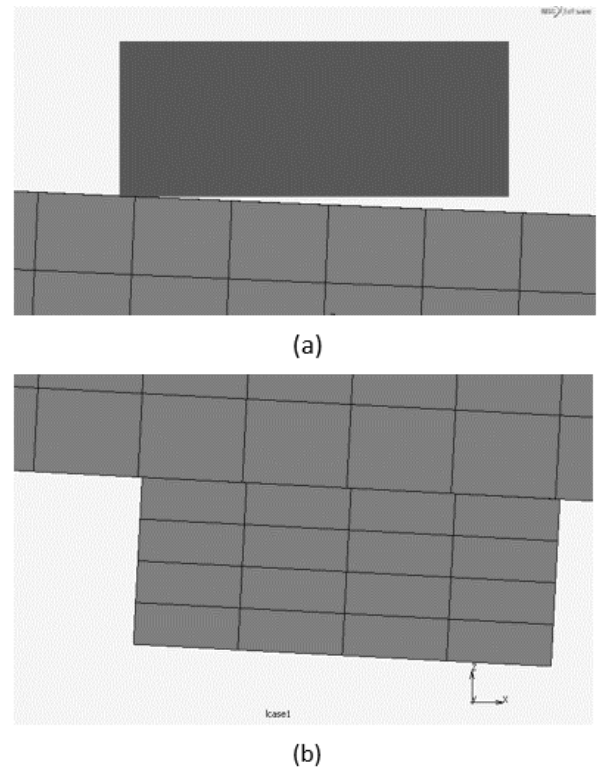


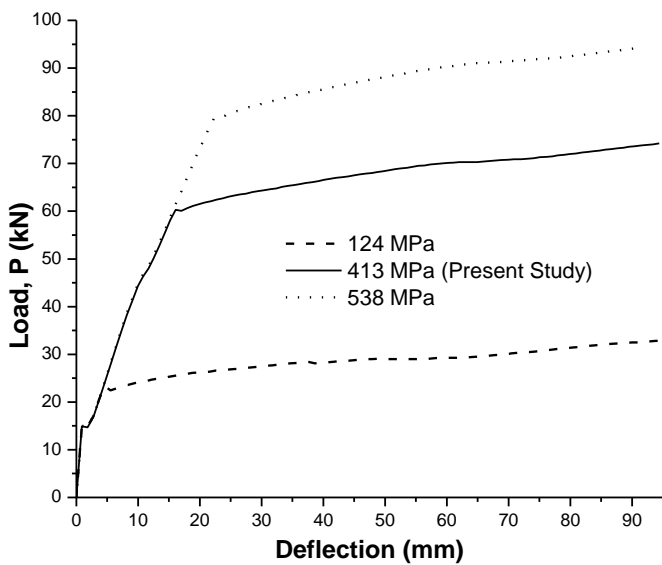
Figure 14. Contact behavior (a) at the loading point (b) at support.

### 5.4 Parametric Study

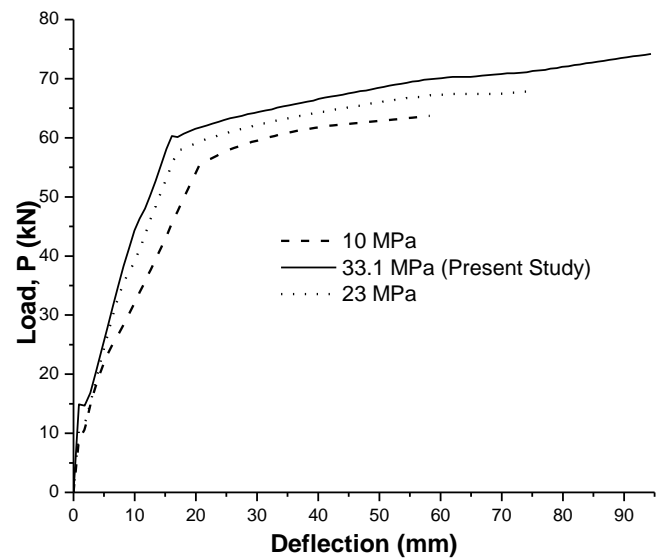
The FEA model was observed to have effectively represented the experimental results and this is observed in the same load and boundary conditions and this further led to the analysis of the steel reinforcement’s yield strength using 124 MPa and 538 MPa to determines its effects on the structural behavior of RC beam, concrete compressive strength using 10 MPa and 23 MPa, and tensile model of the RC beams as shown in Figure 2 using different negative elastic modulus values,  $E$ , at 1 MPa and 19058.9 MPa.

Figure 15 (a) shows the effect of steel reinforcement yield strength on load-deflection behavior of the beam and the maximum load was observed to be getting higher as the yield strength was increasing. Meanwhile, the beam deflection was reducing as the concrete compressive strength was decreasing as shown in Figure 15 (b) and the program stopped running when a crushing strain of 0.003 was reached. Moreover,

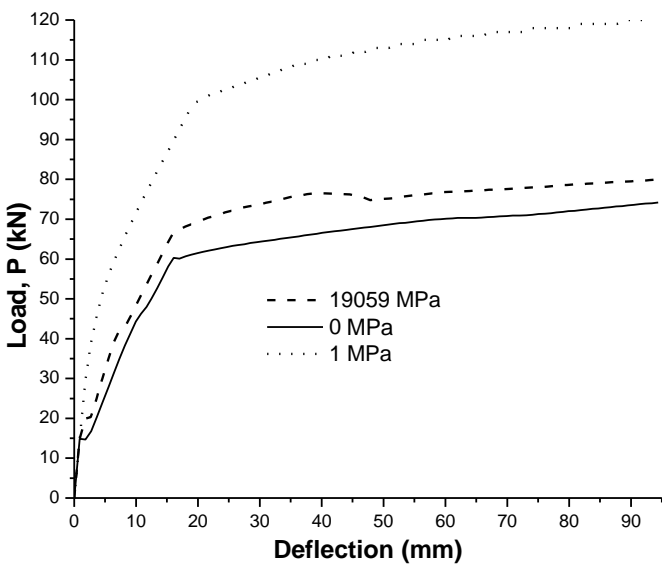
the effect of the tensile model on the structural behavior of the RC beam is presented in Figure 15 (c) and this is reflected in the negative elastic modulus which was equal to 1 MPa, after cracking, the value of the uniaxial tensile strength was constant and the load-deflection curve became higher. The same phenomenon was recorded at 19059 MPa with the load-deflection observed to have slightly increased.



(a)



(b)



(c)

Figure 15. Parametric study: (a). The effect of yield strength, (b) The effect of concrete compressive strength, and. (c) The effect of the tensile strength model.

## 6 CONCLUSION

This study analyzed the embedded model of reinforcement inside concrete elements using MSC MARC/MENTAT. Moreover, contact analysis was conducted between the deformable elements of concrete and steel as well as the loading point. The results showed the load-deflection response of the FEA model had good agreement with the experimental findings and a slip was found to be existing between the support and loading point. The parametric study conducted also showed load-deflection significantly increased with an increment in steel reinforcement yield strength and the same was recorded for concrete compressive strength but the deflection was observed to be getting smaller as the compressive strength decreases because the crushing strain has been reached. Meanwhile, the concrete tension model was also the same with the experimental results with the tensile strength observed to have been lost after the tensile stress has been reached.

## DISCLAIMER

The authors declare no conflict of interest.

## ACKNOWLEDGMENTS

The author is grateful for the critical comments of anonymous reviewers and the Editor, which helped in improving the quality of this paper

## REFERENCES

Buckhouse, E.R., 1997. External flexural reinforcement of existing reinforced concrete beams using bolted steel channels.

Dahmani, L., Khennane, A. and Kaci, S., 2010. Crack identification in reinforced concrete beams using ANSYS software. *Strength of materials*, 42(2), pp.232–240.

Dawari, V.B. and Vesmawala, G.R., 2014. Application of nonlinear concrete model for finite element analysis of reinforced concrete beams. *International Journal of Scientific & Engineering*

*Research*, 5(9).

Halahla, A., 2019. Identification of Crack in Reinforced Concrete Beam Subjected to Static Load Using Non-linear Finite Element Analysis. *Civil Engineering Journal*, 5(7), pp.1631–1646.

Kachlakev, D.I., Miller, T.H., Potisuk, T., Yim, S.C. and Chansawat, K., 2001. *Finite element modeling of reinforced concrete structures strengthened with FRP laminates*. Oregon. Dept. of Transportation. Research Group.

Korol, E. and Tejchman, J., 2011. Experimental and theoretical studies on size effects in concrete and reinforced concrete beams. *CMM-2011—Computer Methods in Mechanics, Warsaw, Poland*, 9, p.12.

Ling, J.H., Chan, L.L., Leong, W.K. and Sia, H.T., 2020. The Development of Finite Element Model to Investigate the Structural Performance of Reinforced Concrete Hollow Beams. In: *Journal of the Civil Engineering Forum*. pp.171–182.

Logan, D.L., 2000. *A first course in the finite element method using Algor*. Brooks/Cole Publishing Co.

Marc, M.S.C., 2010a. Volume A: Theory and user information. *MSC. Software Corporation*.

Marc, M.S.C., 2010b. Volume B: Element Library. *MSC. Software Corporation*, pp.113–661.

Marc, M.S.C., 2012. Volume B: Element Library, *MSC. Software Corporation*.

Markou, G. and Papadrakakis, M., 2012. An efficient generation method of embedded reinforcement in hexahedral elements for reinforced concrete simulations. *Advances in Engineering Software*, 45(1), pp.175–187.

Öchsner, A. and Öchsner, M., 2016. *The finite element analysis program MSC Marc/Mentat*. Springer.

Özcan, D.M., Bayraktar, A., Şahin, A., Haktanir, T. and Türker, T., 2009. Experimental and finite element analysis on the steel fiber-reinforced concrete (SFRC) beams ultimate behavior.

*Construction and Building Materials*, 23(2), pp.1064–1077.

Saifullah, M., Nasir, U. and Udin, S., 2011. Experimental and analytical investigation of flexural behavior of reinforced concrete beam.

Słowik, M. and Smarzewski, P., 2012. Study of the scale effect on diagonal crack propagation in concrete beams. *Computational Materials Science*, 64, pp.216–220.

Smarzewski, P., 2016. Numerical solution of reinforced concrete beam using arc-length method. *Biuletyn Wojskowej Akademii Technicznej*, 65(1).

Suku, Y.L. and Je, K., 2020. Modeling and Analysis of the Effect of Holes in Reinforced Concrete Column Structures. In: *Journal of the Civil Engineering Forum*. pp.27–36.

Tavárez, F.A., 2001. *Simulation of behavior of composite grid reinforced concrete beams using explicit finite element methods*. University of Wisconsin--Madison.

Tjitradi, D., Eliatun, E. and Taufik, S., 2017. 3D ANSYS Numerical Modeling of Reinforced Concrete Beam Behavior under Different Collapsed Mechanisms. *International Journal of Mechanics and Applications*, 7(1), pp.14–23.

Vasudevan, G., Kothandaraman, S. and Azhagarsamy, S., 2013. Study on non-linear flexural behavior of reinforced concrete beams using ANSYS by discrete reinforcement modeling. *Strength of materials*, 45(2), pp.231–241.

Wolanski, A.J., 2004. *Flexural behavior of reinforced and prestressed concrete beams using finite element analysis*.

**APPENDIX****Crack initiation**

The gross moment of inertia

$$I_G = \frac{1}{12}bh^3 = 2022884728 \text{ mm}^4$$

The modulus of elasticity of the concrete:

$$E_c = 27227 \text{ Mpa}$$

The modulus of rupture

$$f_t = 0.7\sqrt{f_c} = 4.02 \text{ Mpa}$$

The crack initiation moment based on concrete gross section properties

$$M_{cr} = \frac{f_t I_G}{h/2} = 35573.03 \text{ kN/mm}$$

Loading to crack initiation

$$P_{cr} = \frac{M_{cr}}{1524} = 23.34 \text{ kN}$$

**Ultimate Strength Calculations for Cracked Section**

For ultimate load, the carrying strength capability tension stress in the concrete was assumed to be nonexistent and

the maximum compressive strain assumed to be equal  $\varepsilon_u = 0.003$ .

The steel reinforcement in tension is assumed to be yielding.

Moment Reduction factor  $\phi$  set equal to 1.0 to compute Ultimate moment,

Uniform distribution rectangular stress block, stress intensity factor  $\beta_1$

According to SNI 2847:2013 10.2.7.3 for  $f_c' 28 \text{ MPa}$

$$\begin{aligned} \beta_1 &= 0.85 - \frac{0.05(f_c' - 28)}{7} \\ &= 0.85 - \frac{0.05(33.1 - 28)}{7} \\ &= 0.81 \geq 0.65 \end{aligned}$$

$$a = \frac{A_s f_y}{0.85 f_c' b} = 34.8 \text{ mm}$$

$$c = \frac{a}{\beta_1} = 42.8 \text{ mm}$$

$$\begin{aligned} \frac{c}{d} = \frac{\varepsilon_u}{\varepsilon_u + \varepsilon_y} \Rightarrow \varepsilon_t = \varepsilon_u \frac{d_t - c}{c} &= 0.003 \frac{393.7 - 42.8}{42.8} \\ &= 0.024596 > \varepsilon_y \end{aligned}$$

-- the steel yielding assumption is correct

$$\phi M_u = A_{st} f_y \left( d - \frac{a}{2} \right) = 93742248.6 \text{ Nmm}$$

The maximum loading,  $P_0 = \frac{\phi M_u}{1524} = 61.5 \text{ kN}$

[This page is intentionally left blank]